Mexican Journal of Biotechnology 2023, 8(1):1-20

Journal homepage:www.mexjbiotechnol.com

ISSN:2448-6590

ORIGINAL RESEARCH

Antibacterial behavior and bacterial resistance analysis of *P. aeruginosa* in contact with copper nanoparticles

Comportamiento antibacteriano y análisis de resistencia bacteriana de *P. aeruginosa* al contacto con nanopartículas de cobre

Karen Guadalupe Quintero-Garrido[1,2], Fátima Berenice Ramírez-Montiel[1,3], Marilú Chávez-Castillo[2], Yolanda Reyes-Vidal[1], Francisco Javier Bacame-Valenzuela[1], Felipe Padilla-Vaca[3], Lourdes Palma-Tirado[4], Miriam Estevez[5], Beatriz Liliana España-Sánchez[1]*

[1]Centro de Investigación y Desarrollo Tecnológico en Electroquímica CIDETEQ. S.C., Parque Tecnológico Querétaro s/s Sanfandila, Pedro Escobedo, Querétaro. C. P. 76703, Mexico. [2]Universidad Tecnológica Emiliano Zapata del Estado de Morelos. Av. Universidad Tecnológica No. 1, Col. Palo Escrito, Emiliano Zapata, Morelos. C. P. 62760, Mexico. [3]Departamento de Biología, División de Ciencias Naturales y Exactas, Universidad de Guanajuato, Noria alta s/n, Guanajuato, Guanajuato. C. P. 36050, Mexico. [4]Instituto de Neurobiología, Universidad Nacional Autónoma de Mexico. Boulevard Juriquilla No. 3001, Juriquilla, Querétaro. C. P. 76230, Mexico. [5]Centro de Física Aplicada y Tecnología Avanzada, Universidad Nacional Autónoma de Mexico, Boulevard Juriquilla 3001, Querétaro, Qro., 76230, Mexico.

*Corresponding author
E-mail address: lespana@cideteq.mx (B.L. España-Sánchez)

Article history:
Received: 31 October 2022 / Received in revised form: 1 December 2022 / Accepted: / 2 December 2022 / Published online: 3 January 2023.
https://doi.org/10.29267/mxjb.2023.8.1.1

ABSTRACT

The present study describes the antibacterial behavior and the bacterial resistance analysis of extremophile *Pseudomonas aeruginosa* in contact with copper nanoparticles (CuNPs). For this purpose, green synthesis of CuNPs was performed by combined ultrasound-assisted and chemical reduction methods, obtaining semispherical CuNPs ranging from *ca.* 4-9 nm. Antibacterial activity (AA) of biosynthesized CuNPs demonstrates an antibacterial inhibition of 85 % (LD_{85}) at 400 µg/mL and a minimum bactericidal concentration (MBC) of 800 µg/mL after 3 h of contact. Bacterial adaptation in contact with CuNPs was observed through the consecutive exposition of microorganisms, presenting a significant increase of LD_{85} values from 400 µg/mL to 6400

µg/mL after 11 expositions. This behavior demonstrates the bacterial growth adaptation with high-dose of CuNPs. The bacterial resistance mechanism was determined through the overproduction of pyocyanin, associated with oxidative stress events, the genomic polymorphism of resistant bacteria obtained by PCR-RAPDs, and the morphological interaction between *P. aeruginosa* and CuNPs evidenced by transmission electron microscopy (TEM) micrographs. Our results suggest that under controlled CuNPs exposition, extremophile *P. aeruginosa* can generate bacterial resistance mechanisms, an important issue for the effective design of antimicrobial nanomaterials.

Keywords: antimicrobial nanomaterials, bacterial tolerance, copper nanostructures.

RESUMEN

El presente trabajo describe el comportamiento antibacteriano y el análisis de resistencia bacteriana de *Pseudomonas aeruginosa* extremófila al contacto con nanopartículas de cobre (CuNPs). Para tal efecto, se realizó la síntesis verde de CuNPs asistida por ultrasonido con la reducción química, obteniendo CuNPs que van desde los 4 a 9 nm. La actividad antibacteriana (AA) de las CuNPs biosintetizadas demostraron una LD_{85} de 400 µg/mL y una concentración mínima bactericida (CMB) de 800 µg/mL, después de 3 h. La adaptación bacteriana en contacto con CuNPs se observó a través de la exposición consecutiva de los microorganismos, presentando un aumento significativo de los valores de CMI de 400 µg/mL a 6400 µg/mL después de 11 exposiciones. Este comportamiento demuestra la adaptación al crecimiento bacteriano con dosis altas de CuNPs. El mecanismo de resistencia bacteriana se determinó a través de la sobre producción de piocianina, asociada a eventos de estrés oxidativo, el polimorfismo genómico de bacterias resistentes obtenido por PRC-RAPDs y la interacción de las CuNPs con *P. aeruginosa* evidenciados mediante análisis microscópico. Nuestros resultados sugieren que, la exposición controlada de CuNPs, *P. aeruginosa* puede generar mecanismos de resistencia bacteriana, un tema importante para el diseño efectivo de nanomateriales antimicrobianos.

Palabras clave: nanomateriales antimicrobianos, tolerancia bacteriana, nanoestructuras de cobre.

1. INTRODUCTION

The uncontrolled development of bacterial resistance by pathogenic microorganisms represents an important problem for public health due to the insufficient ability of antibiotics to combat the new generation of resistant microorganisms (Fariña, 2016; Jones & Pfaller, 1998). To solve this problem, current strategies to develop novel antimicrobials are focused on applying nanotechnology (Mubeen *et al.*, 2021). In particular, metal-based nanoparticles (NPs) obtained from green sources have emerged as a novel tool to produce functional antimicrobial nanomaterials due to their capacity to avoid the growth and propagation of a broad spectrum of microorganisms such as bacteria, fungi, and viruses (Sánchez-Lopez *et al.*, 2020). The antimicrobial functionality of NPs such as silver, copper, zinc oxide, and titanium dioxide, among others, lies in their combined intrinsic physicochemical properties, their high surface reactive area

associated with the low NPs size (1-10 nm), and their non-specific bacterial toxicity mechanisms (Amaro *et al.*, 2021). Furthermore, it has been claimed that NPs display multiple antibacterial mechanisms, including the combined bacterial cell wall damage, alteration in the protein synthesis, DNA mutations, and the overproduction of reactive oxygen species (ROS), resulting in bacterial death (Niño-Martínez *et al.*, 2019).

Despite the high antibacterial efficacy of nanoscale materials, recent studies have demonstrated the possibility of generating bacterial resistance mechanisms in contact with low-dose NPs (McNeilly *et al.*, 2021; Panáček *et al.*, 2018). In particular, silver NPs (AgNPs) can rapidly develop resistance to their intrinsic antibacterial behavior, showing an increase in the minimum inhibitory concentration (MIC) values after repeated exposure (20 expositions) against Gram-negative *E. coli* and *P. aeruginosa*. As a result, a combined NPs aggregation around the bacterial wall and the overproduction of metabolites from the extracellular matrix (ECM), such as flagellin, suggest the possible development of defense mechanisms by the constant interaction with the nanomaterial (Panáček *et al.*, 2018). On the other hand, the combined copper oxide NPs and Cu ions in solution can stimulate the horizontal gene transference in *E. coli* and *Pseudomonas putida* through the overproduction of ROS species. As a result, the overexpression of specific genes associated with oxidative stress, membrane repair, and ECM metabolites are detected under low-dose Cu species (Zhang *et al.*, 2019).

Most reports on the antibacterial behavior of NPs described the material's susceptibility to contact with conventional microorganisms used as models, such as *Escherichia coli* and *Staphylococcus aureus*. However, little is known about the behavior of extremophile microorganisms in contact with nanomaterials. Bacterium extremophiles are a group of microorganisms capable of surviving under extreme growth conditions due to their peculiar metabolisms, such as temperature, pressure, ionic species or metals, and radiation. This behavior commonly allows for the production of biomolecules such as metabolites (pigments, lipids, or proteins) concerning their potential industrial biotechnological applications, such as bioremediation or energy-renewable production (Romano, *et al.*, 2022). In particular, *Pseudomonas aeruginosa* has been described as an opportunist pathogen with high virulence factors and bacterial resistance (included in the ESKAPE list) and is considered one of the most aggressive microorganisms associated with several infectious diseases (Alonso *et al.*, 2020). In addition, due to their versatile metabolism, they can be isolated from complex carbon sources such as industrial effluents and gain important attention in ambient processes (Bacame-Valenzuela *et al.*, 2020). An important characteristic of extremophile *P. aeruginosa* is the production of a redox-active phenazine derivative denoted as pyocyanin as a response to the bacterial exposition under extreme growth conditions, associated with the overproduction of ROS species (Muller & Merrett, 2014; Whooley & McLoughlin, 1982), which is commonly observed by the characteristic greenish-blue coloration. According to the above, the expression of pyocyanin in *P. aeruginosa* could represent a relevant parameter to detect bacterial stress associated with the interaction with metal-based nanomaterials.

Therefore, our work describes the antibacterial behavior and the bacterial resistance assays of extremophile *P. aeruginosa* NEJ08 in contact with CuNPs, aiming to determine the possible bacterial adaptation mechanisms induced by consecutive contact with

CuNPs. For this purpose, CuNPs were biosynthesized by combined ultrasound-assisted and chemical reduction methods with the extract of blueberries (*Vaccinium corymbosum*). Also, the antibacterial activity (AA) of CuNPs was performed at different NPs amounts, and the consecutive bacterial exposition determined the bacterial resistance analysis to NPs. Three targets were studied to determine the possible bacterial resistance of *P. aeruginosa*: the pyocyanin production associated with the oxidative stress event, the genomic mutations through the PCR-RAPDs analysis of susceptible and resistant bacteria, and the morphological changes of the bacterial structure by the interaction with CuNPs.

2. MATERIALS AND METHODS

2.1. Synthesis of CuNPs

CuNPs were synthesized using copper sulfate pentahydrate (Sigma Aldrich) as a metal precursor and *Vaccinium corymbosum* extract (blueberries) as a reducing/stabilizer agent for NPs formation (purchased from the local market of Querétaro, Mexico). Briefly, 16 g of blueberries were washed with deionized water, mixed with 20 mL water/30 mL ethanol 70 %, and filtered with a Whatman filter (1 µm). The pH of the extract was adjusted to 2 with ascorbic acid (0.5 M). Then, 50 mL of Copper sulfate (0.15 M) was mixed with 50 mL of blueberry extract and sonicated with a Q500 *Qsonica* equipment (20 kHz, 80 % amplitude) for 10 min at room temperature. Next, CuNPs were washed with water/ethanol, centrifuged (6000 rpm, 15 min), and dried to obtain the CuNPs powder. To corroborate the CuNPs formation, 1 mg of powder was dispersed in 50 mL ethanol. A drop was placed in a copper grid (300 mesh) coated with lacey carbon and observed by Transmission Electron Microscopy (TEM). Micrographs were obtained using a Jeol 1010 at 80 kV.

2.2. Antibacterial activity of CuNPs against *P. aeruginosa*

A strain of extremophile *Pseudomonas aeruginosa* NEJ08 (GenBank MZ835665) was isolated from wastewater obtained from the maize industry in Ambiental Microbiology Lab (CIDETEQ SC.) and used as a Gram-negative bacteria model. Microorganisms were growth in Mueller Hinton agar (MH, BD Bioxon), employing a bacterial inoculum of 1^x10^6 colony-forming unit (CFU) per mL. Phosphate buffer solution (PBS) was employed for NPs suspension, and Tween 80 (1 wt. %) purchased from Merck was incorporated into PBS as a dispersant agent.

Different CuNPs suspension (100, 200, 400, 800, 1600, 3200 and 6400 µg/mL) were evaluated by microdilution method (Fig. 1). A mix of 1:1 bacterial/CuNPs suspension was placed in Eppendorf tubes and incubated for 1 h and 3 h at 37 °C. After the interaction, an aliquot (50 µL) was plated in Mueller Hinton plates and incubated for 16 h at 37 °C. In three independent experiments, duplicated survival bacterial recovery (antibacterial

activity, AA) was calculated according to our previous work (España-Sánchez *et al.*, 2018).

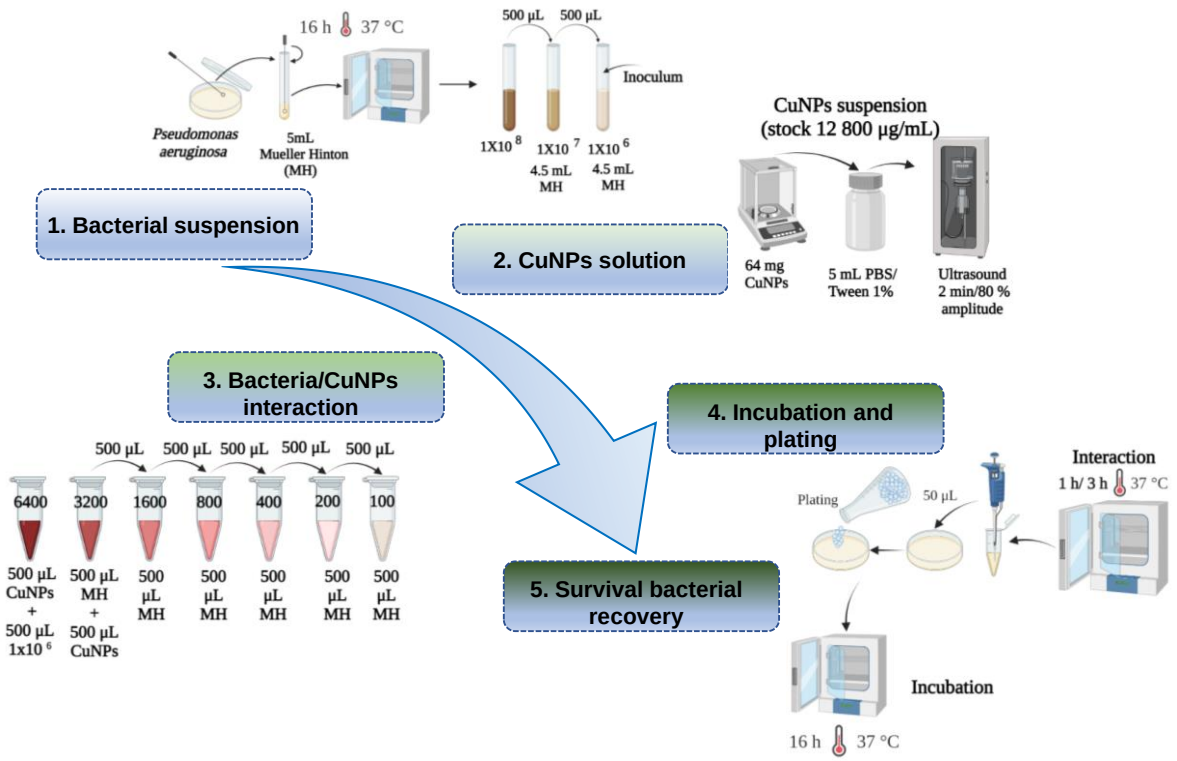

Fig. 1. Schematic representation of antibacterial assays of *P. aeruginosa* in contact with CuNPs by microdilution method.

2.3. Bacterial resistance assay of *P. aeruginosa* with consecutive CuNPs exposition

The consecutive exposition of *P. aeruginosa* to CuNPs was performed by selecting AA results. For this purpose, we select the CuNPs plate that shows the *ca.* 85 % of bacterial inhibition (considered as the LD_{85}) and the CuNPs plate that shows the complete bacterial growth (denoted as the minimum bactericidal concentration, MBC). The bacterial recovery was performed in the LD_{85} plate. After bacteria/CuNPs exposition, the bacteria recovered were plated in an MH plate and incubated for 16 h at 37 °C. According to the AA assay, eleven consecutive expositions of *P. aeruginosa* NEJ08 with CuNPs were performed to evaluate the LD_{85} value changes attributed to the possible bacterial adaptation to the NPs exposition.

2.4. Pyocyanin quantification from *P. aeruginosa* growth

The pyocyanin concentration was determined by the modified method reported by Bacame-Valenzuela *et al.*, (2020). Luria Bertani agar was prepared and sterilized in an

autoclave, and 25 mL of agar was placed in Petri dishes. Subsequently, they were massively inoculated with *Pseudomonas aeruginosa* NEJ08 and incubated at 30 °C for 48 h. The agar was cut into 1 cm squares and placed in a bottle, and 10 mL of sterile water was added. The mixture was vigorously shaken, recovered the supernatant, and centrifuged at 7000 rpm for 5 min. A 1:1 mixture of the supernatant and chloroform was made, and the organic phase was recovered with the blue pigment. In addition, a 1:1 mixture of the organic phase with 0.2 N hydrochloric acid was obtained. After shaking, the aqueous phase with the red pigment was recovered. The absorbance measured in a UV-Vis spectrophotometer (Genesys™ 10S, Thermo Scientific, WI, USA) was determined at 520 nm. The absorbance was multiplied by the factor 17.1 to obtain µg mL−1 of pyocyanin. This factor represents the pyocyanin quantification in their acidic form at 520 nm, according to the equation reported by El-Fouly *et al.*, (2015); Essar *et al.*, (1990).

2.5. Genomic DNA analysis of *P. aeruginosa* exposed to CuNPs

Genomic analysis of *P. aeruginosa* NEJ08 (susceptible and resistant) was performed by DNA isolation using a Wizard® Genomic DNA purification kit (Promega), following the protocol for Gram-negative bacteria extraction. Briefly, 5 mL of Mueller Hinton broth (MH) with *P. aeruginosa* grew at 37 °C for 16 h. All the microorganisms were centrifuged at 13,000 rpm for 2 min, and the MH media was removed. Bacteria were suspended in 450 µL of EDTA 50 mM and 20 µL of lysozyme, incubated at 37 °C for 30 min, and centrifuged. Afterward, 600 µL of nuclei lysis solution was placed in the bacteria tube and incubated at 80 °C for 5 min. The sample was tempered, and 3 µL of Rnase was mixed and incubated at 37 °C for 30 min. Protein precipitation solution (200 µL) was vigorously mixed with the bacteria tube, incubated in ice, and centrifuged for 3 min. The final DNA supernatant was transferred to another Eppendorf tube with 600 µL isopropanol for the DNA precipitation. DNA quantification was performed with 20 µL of DNA mixed with 70 µL of distilled water with a UV spectrophotometer BIOBASE BK-UV1800PC at 260 and 280 nm, according to the equation:

$$50 \times Abs_{260} = \text{DNA concentration (ng/µL)}$$

Also, the DNA quality was evaluated by agarose gel electrophoresis 1 %.

2.6. PCR-RAPDs of *P. aeruginosa* exposed to CuNPs

The effect of the DNA of *P. aeruginosa* after consecutive bacterial exposition to CuNPs was evaluated by random amplified polymorphic DNA-PCR methodology (RAPDs). For this purpose, five 10-bases primers were used to evaluate the changes in the DNA molecular weight after the interaction with CuNPs (786, OPQ14, OPR12, OPA11, and OPE06). The primer sequence is presented in Table 1. The PCR reactions were performed with 5 µL of primer, 10 µL of GoTaq, 20 µL of distilled water, and 2 µL of DNA (30 ng). Reactions were carried out in a thermal cycler Life ECO TC96/G/H(b)C, including 1 cycle (5 min, 95 °C) for the initial DNA denaturalization; 40 cycles (95 °C for 1 min/36 °C for 1 min/72 °C for 2 min) for the DNA amplification and finally, 1 cycle at 72 °C for 5

min to complete the DNA extension. PCR products were evaluated by electrophoresis using agarose gel 1 %, employing a TrackIt™ marker as molecular weight reference. Agarose gels were photographed in a BIOBASE photodocumentator BK-AG100, and the images were processed in the GelAnalyzer software.

2.7. Morphological analysis of *P. aeruginosa* exposed to CuNPs by TEM

Morphology of *P. aeruginosa* with low-dose (200 µg/mL) and high-dose (800 µg/mL) of CuNPs was evaluated by transmission electron microscopy (TEM) and compared with a reference without NPs. Bacterial growth interacted with CuNPs and was processed by three steps: prefixation, dehydration, and embedded in epoxy resin. First, bacterial/CuNPs interactions were mixed with glutaraldehyde 1 % for 1 h. Subsequently, samples were washed 4-5 times with sodium cacodylate solution (0.1 M). Next, samples were mixed with glutaraldehyde 1.5 % for 2 h and washed again with sodium cacodylate solution. Next, centrifuged samples were stained with 1 mL osmium tetraoxide (1 %), and stored for 24 h, at 4 °C. Samples were washed and dehydrated for 10 min with ethanol 50 %, 70 %, 96 %, and absolute ethanol, respectively. Then, the supernatant was removed, and 1 mL of propylene oxide was placed for 10 min at room temperature (three times). Finally, samples were embedded in epoxy resin (EPON 812) mixed 1:1 with propylene oxide and stored at room temperature for 48 h. Each sample was placed in molds and dried for 72 h at 60 °C. The bacterial sample was cut un a microtome with an average thickness of *ca.* 60 nm and placed in nickel grids (300 mesh) for TEM observation, employing a Jeol 1010 at 80 kV.

3. RESULTS

Fig. 2 presents the TEM micrographs of the semispherical and monodispersed CuNPs obtained, with an average diameter of *ca.* 4-9 nm, associated with the combined ultrasound-assisted method to NPs synthesis and the capacity of *Vaccinium corymbosum* extract (blueberries) to reduce the copper salt.

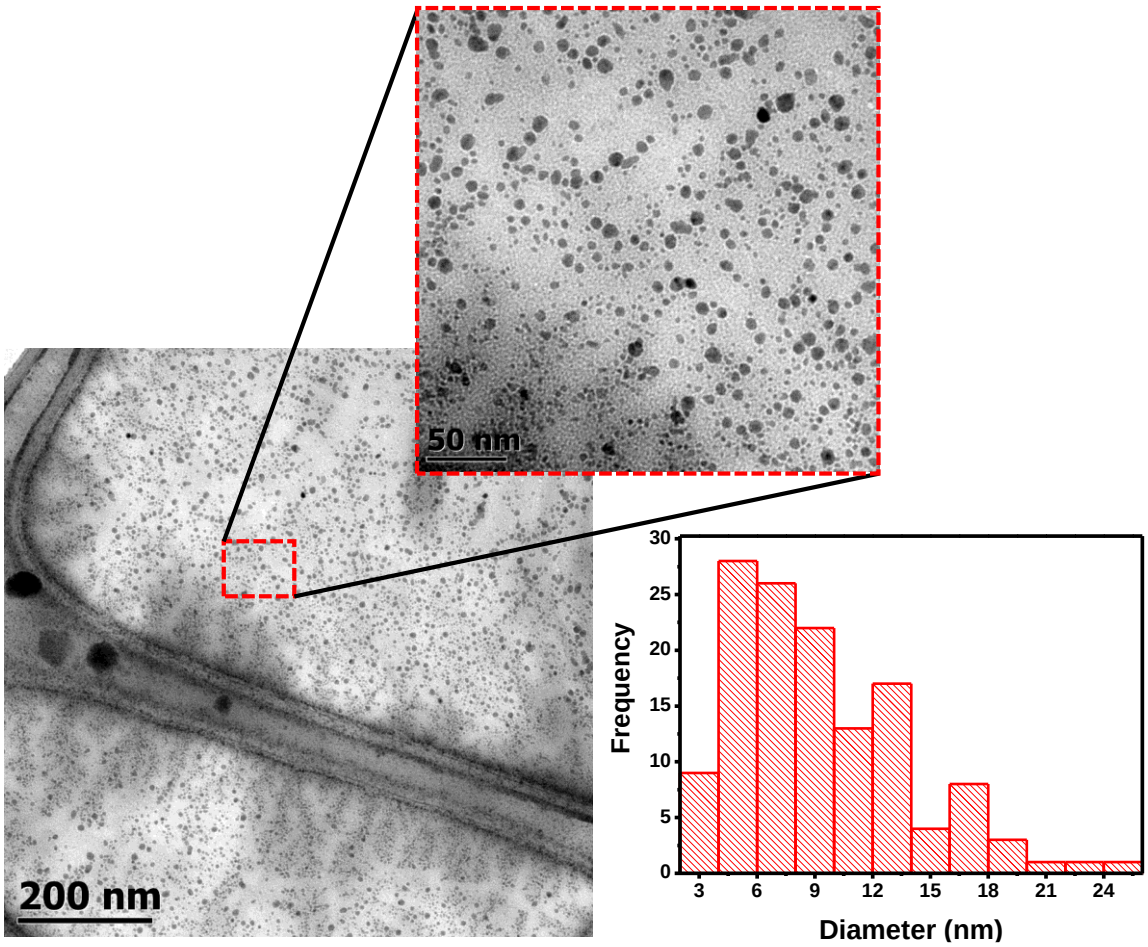

Fig. 2. TEM micrographs of copper nanoparticles (CuNPs) synthesized by ultrasound-assisted method, using *Vaccinium corymbosum* extract as reducing/stabilizer agent. The inset represents the histogram of CuNPs.

Antibacterial activity (AA) of biosynthesized CuNPs was performed (Fig. 3) against *P. aeruginosa* NEJ08 at a short contact time (1 h and 3 h). At 200 µg/mL, the AA is *ca.* 20 % and 80 %, respectively, while from 400 µg/mL, the complete AA behavior is observed in both times evaluated.

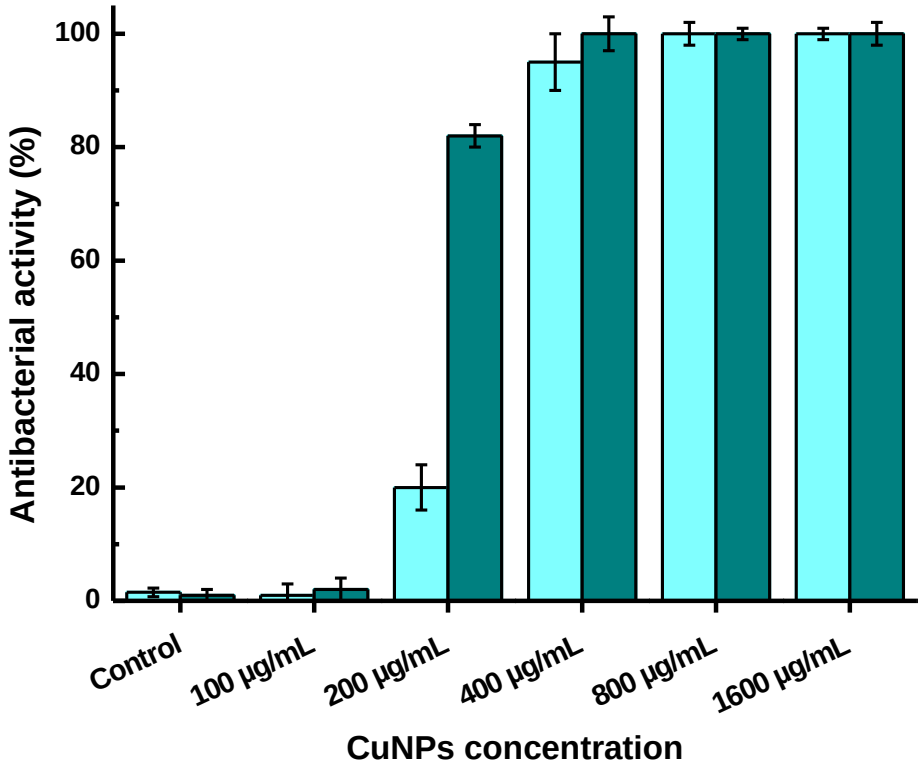

Fig. 3. Antibacterial activity (AA) of *P. aeruginosa* NEJ08 after 1 h (light cyan) and 3 h (dark cyan) of contact with different concentrations of CuNPs.

To explore the possible bacterial adaptation to CuNPs, consecutive bacteria/CuNPs exposition was performed, aiming to determine changes in the LD_{85} values by the contact with different NPs concentrations (as shown in Fig. 4). Initially, *P. aeruginosa* demonstrates a LD_{85} value of 400 µg/mL, denoted as susceptible (initial bacterial/CuNPs exposition). However, after the 1 exposition with CuNPs, a slight decrease of LD_{85} is presented, associated with the known susceptibility of the microorganism to the metal-based antimicrobials (Evans & Kavanagh, 2021). After 3-4 expositions, the LD_{85} value increases to 800 µg/mL; from 5-10 expositions, the increase of the LD_{85} is ca. 3200 µg/mL; after the 11 expositions, the LD_{85} is *ca.* 6400 µg/mL, considered resistant.

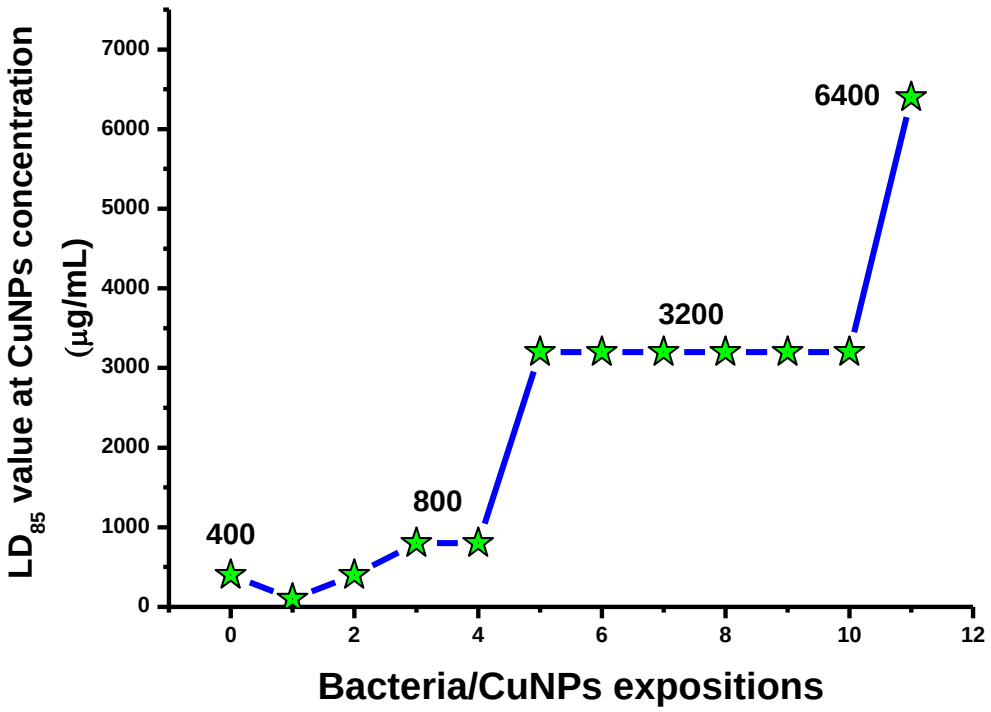

Fig. 4. Bacterial resistance assays of *P. aeruginosa* NEJ08 after consecutive expositions with CuNPs.

Therefore, to evaluate the possible development of the bacterial adaptation mechanism of extremophile *P. aeruginosa* in contact with CuNPs, we evaluate three specific targets: the production of pyocyanin (as a metabolite of the ECM associated with oxidative stress), the genetic modification expressed by PCR-RAPDs with primers associated with bacterial damage, and the morphological analyses of *P. aeruginosa* by TEM micrographs. Fig. 5 shows the pyocyanin production from *P. aeruginosa* plates at lower CuNPs concentration (25, 50, and 100 µg/mL, respectively), with representative photographs that shows the characteristic green color of plates. Bacterial control shows a slight pyocyanin production (*ca*. 0.43 µg/mL). However, the interaction with 25 µg/mL of CuNPs increases pyocyanin production by *ca.* 0.98 µg/mL. In addition, 50 and 100 µg/mL interaction produces *ca.* 0.90 µg/mL of pyocyanin, showing the complete bacterial growth in the MH plates. From 200 µg/mL, pyocyanin decreased significantly, attributed to the drastic decrease in plate colony growth (close to the LD_{85} value).

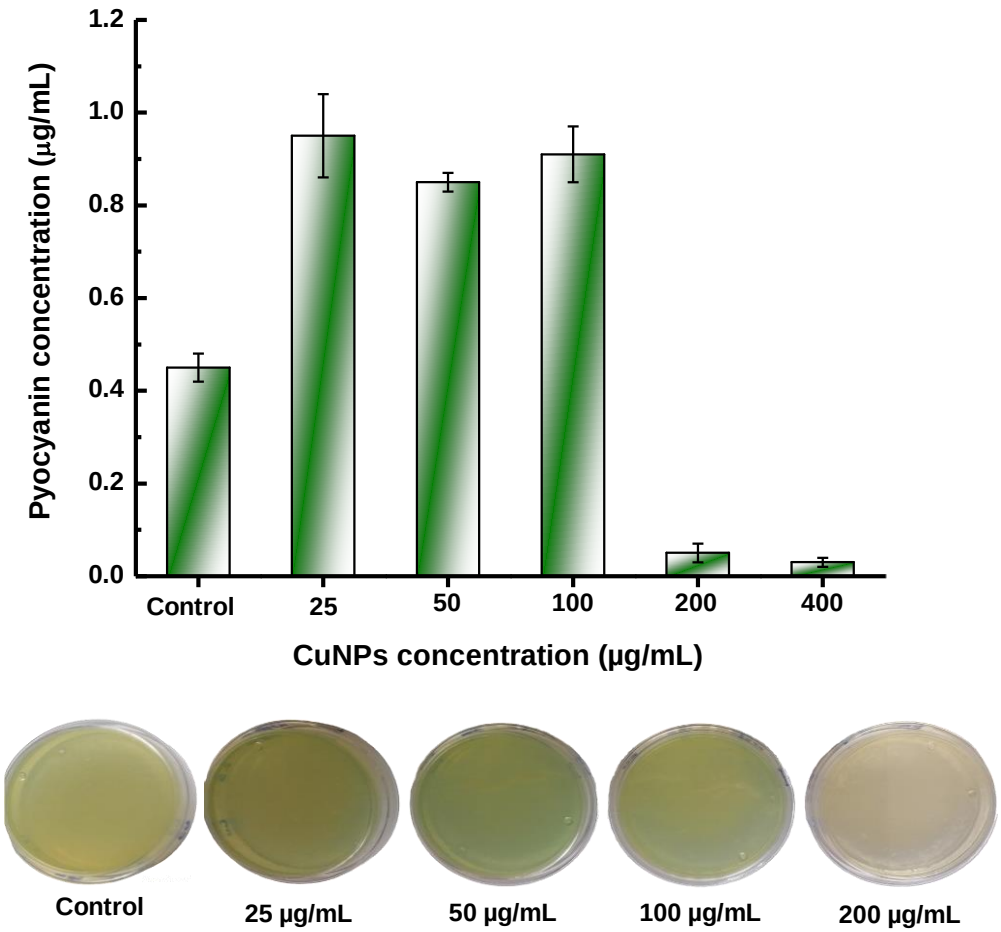

Fig. 5. Pyocyanin quantification assay of *P. aeruginosa* NEJ08 in Mueller Hinton (MH) plates in contact with different concentrations of CuNPs.

To evaluate the genome alterations of the DNA of *P. aeruginosa*, we perform the comparison of the PCR-RAPDs assays between the susceptible bacteria (LD_{85} value of 400 µg/mL) and the resistant bacteria obtained after 11 consecutive expositions to CuNPs (LD_{85} of 6400 µg/mL) through gel agarose electrophoresis, as presented in Fig. 6. The reference of unexposed bacteria (Fig. 6a) shows the bands amplification in three primers: 786 (3 bands located *ca.* 1589, 921, and 636 bps), OPR12 (3 bands located at 2632, 1643, and 1075 bps), and OPA11 (2 bands located at 2741 and 2136 bps). However, the resistant bacteria (Fig. 6b) increase the band amplification in all evaluated primers, indicating a complete polymorphism compared with the susceptible bacteria. The specific band amplification between the susceptible and resistant bacteria is shown in Table 1.

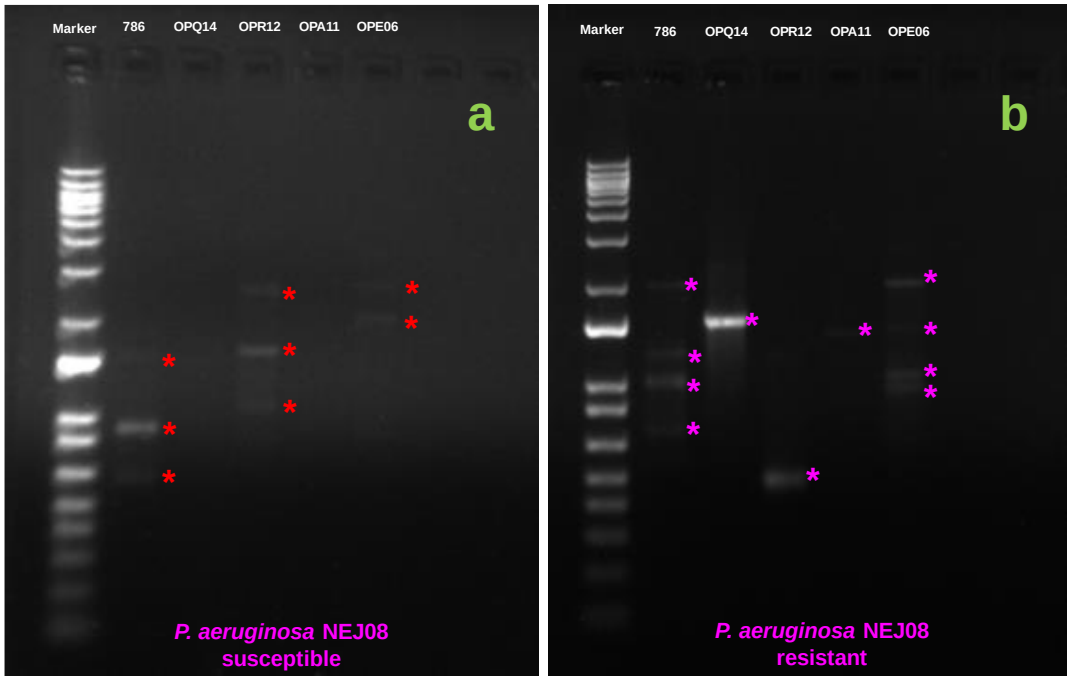

Fig. 6. RAPDs assays of DNA obtained from *P. aeruginosa* NEJ08 susceptible (0 expositions to CuNPs) *vs.* resistant (after 11 expositions with 6400 µg/mL of CuNPs).

Table 1. Primer's sequence employed for the PCR-RAPDs analysis and comparing the bands' amplification expression between *P. aeruginosa* susceptible and resistant to CuNPs.

		***P. aeruginosa* susceptible**			***P. aeruginosa* resistant**		
Primer code	Sequence 5´a 3´	Bands formed	Band number	Molecular weight	Bands formed	Band number	Molecular weight
786	GCG ATCCCCA	3	1	1589	4	1	2105
			2	921		2	1260
			3	636			
						3	1023
						4	708
OPQ-14	GGACGCTTCA	0	-	-	1	1	1609
OPR-12	ACAGGTGCGT	3	1	2632	1	1	500
			2	1643			
			3	1075			
OPA-11	CAATCGCCGT	0	-	-	1	1	1453
OPE-06	AAGACCCCTC	2	1	2741	4	1	2194
						2	1545
			2	2136			

	3	1079
	4	963

The interaction of *P. aeruginosa* induced by contact with CuNPs was evaluated by TEM micrographs (Fig. 7). Untreated extremophile *P. aeruginosa* NEJ08 (Fig. 7a) demonstrates a characteristic bacilli morphology, with an average length of *ca.* 1.5-2 µm. Also, a well-defined bacterial wall is observed, ranging *ca.* 125 nm. The exposition of low-dose of CuNPs (200 µg/mL) is presented in Fig. 7b, showing the slight NPs agglomeration around the bacterial wall. However, no apparent morphology alteration is observed by the NPs exposition. On the other hand, high-dose CuNPs (800 µg/mL) show high NPs agglomeration and the NPs adhesion around the bacterial wall. Additionally, some CuNPs were internalized into the bacterial cytoplasm. It is important to note that the higher NPs interaction with extremophile P. aeruginosa does not alter the characteristic bacterial morphology.

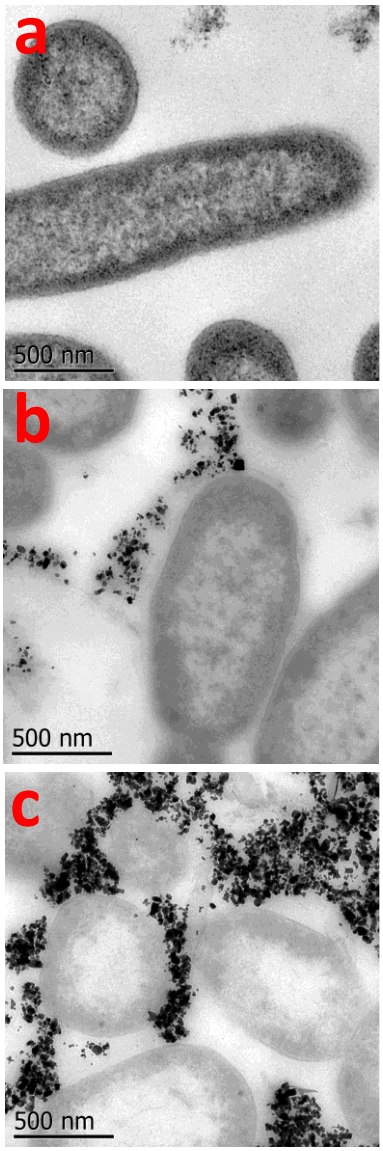

Fig. 7. TEM images of *P. aeruginosa* NEJ08 and their interaction with CuNPs: a) control, b) with 200 µg/mL CuNPs, and c) with 800 µg/mL CuNPs.

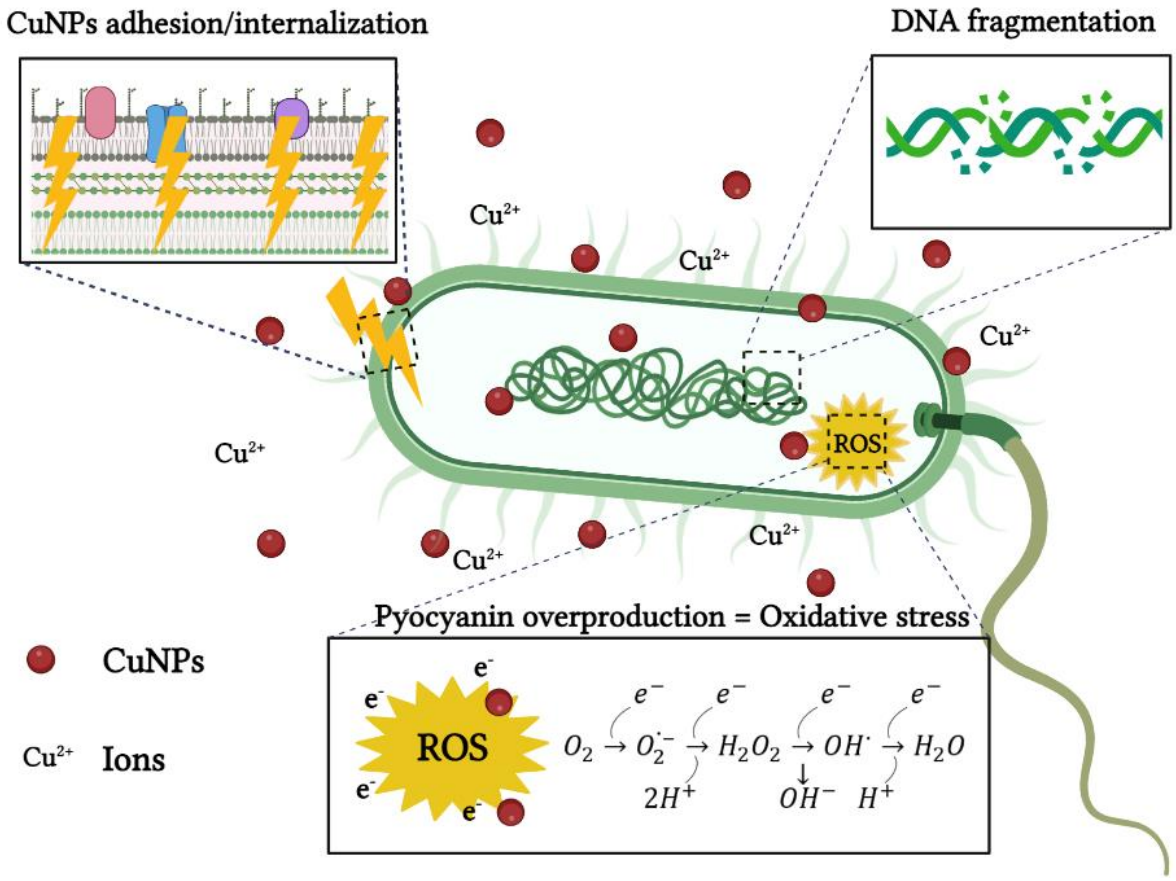

Fig. 8. Bacterial adaptation mechanism of extremophile *P. aeruginosa* NEJ08 induced by the interaction with antibacterial CuNPs. The process includes the combined CuNPs adhesion/internalization in the bacterial wall observed by TEM analysis, the DNA fragmentation obtained from PCR-RAPDs, and the oxidative stress reflected through the pyocyanin production in the ECM of *P. aeruginosa*.

4. DISCUSSION

Green synthesis of metal NPs obtained from combined ultrasound-assisted, and chemical reduction methods represent a low-cost, scalable, and environmentally friendly process to produce nanostructures with antimicrobial characteristics (Guzmán et al., 2019). In this regard, CuNPs synthesis demonstrates the obtaining of semispherical NPs ranging *ca.* 3-9 nm (Fig. 2). The above indicates that the *Vaccinium corymbosum* extract acts as a combined reducing/stabilizer agent, promoting the chemical reduction of $CuSO_4$ salt (Benassai *et al.*, 2021; Keihan *et al.*, 2017). The complete characterization of the CuNPs was previously reported by Humphreys-Salas *et al.* (2022). In addition, the ultrasound

waves catalyze the NPs synthesis and improve the CuNPs dispersion, resulting in a high-controlled size of NPs (Gu *et al.*, 2018).

It has been claimed the broad spectrum of antimicrobial properties of CuNPs against bacteria, fungi, and viruses (Govind *et al.*, 2021; Muñoz-Escobar & Reyes-López, 2020; Salah *et al.*, 2021). In particular, extremophile microorganisms have gained attention due to their capacity to biosynthesize metal NPs under extreme environmental conditions, such as silver NPs (Atalah *et al.*, 2022). However, the potential antibacterial properties and the capacity to generate intrinsic adaptation to the NPs exposition of extremophile microorganisms have not been addressed. Our results indicate that biosynthesized CuNPs demonstrate high antibacterial properties against Gram-negative bacteria associated with the NPs concentration (Fig. 3), higher than reported by Zangeneh *et al.* (2019).

Despite the metal-based nanostructures have demonstrated unique physicochemical properties and a broad spectrum of AA, recent studies have mentioned the development of resistant bacteria in contact with silver NPs (McNeilly *et al.*, 2021; Panáček *et al.*, 2018). Our results suggest that *P. aeruginosa* tends to adapt to the CuNPs environment, with the capacity to grow with high NPs amounts (Fig. 4), and confirm the bacterial adaptation mechanism in contact with CuNPs. It is important to note that extremophiles provide specific metabolic mechanisms to produce biomolecules, which can intervene in bioremediation processes (Marques, 2018), explaining the possibility of adapting bacterial growth under adverse conditions. According to the report by Niño-Martínez *et al.* (2019), the bacterial resistance mechanism produced by the interaction with NPs includes the charge modulation of the external cell wall, the regulation of ion efflux, the generation of metabolites from the extracellular matrix (ECM), the biofilm production and mutations associated with genetic modifications, associates with the alterations of the virulence factors. Despite the low doses of CuNPs not demonstrating changes in bacterial growth, the physiological manifestation of pyocyanin (Fig. 5) indicates the possible oxidative stress induction in *P. aeruginosa* (Hall *et al.*, 2016; Jabłońska *et al.*, 2022). The above is because pyocyanin is a redox pigment considered an important source of reactive oxygen species (ROS), and their overproduction can generate significant alterations in the bacterial structure. It has been reported that low-dose nanomaterials such as zinc oxide and multi-walled carbon nanotubes stimulate the production of bacterial pigments (Jabłońska *et al.*, 2022). According to our results, the low-dose exposition of CuNPs generates stress in the growth of *P. aeruginosa*, suggesting the overproduction of pigments from the ECM as a possible protective mechanism for the bacteria in front of the NPs exposition.

Changes in the band's amplification obtained by the consecutive CuNPs exposition are commonly associated with the genetic variation produced by the horizontal transference of resistant genes (Laehnemann *et al.*, 2014), capable of activating the DNA reparation mechanisms through the DNA polymerase during the PCR reaction, resulting in the inclusion of wrong base pairs and the induction of spontaneous mutations (Tkachenko, 2018). This behavior corroborates the genetic alteration of *P. aeruginosa* under the consecutive CuNPs exposition (Fig. 6), even the bacterial growth at CuNPs concentration is higher than that reported by other references (Ghasemian *et al.*, 2015; Kaur *et al.*, 2016; LewisOscar *et al.*, 2015). According to Bahram, G. E. (2016), Copper oxide NPs

not only affect the bacterial growth of Gram-negative microorganisms but also modify the genomic DNA sequences, producing genomic alteration of bacteria at lower NPs amounts (30-60 µg/mL). As a result, genomic modification of *P. aeruginosa* is presented as a bacterial adaptation mechanism to high-dose NPs in aqueous media. Finally, the morphology of *P. aeruginosa* and their interaction with different doses of CuNPs (Fig. 7) demonstrates that the NPs/bacterial interaction occurs exclusively although the bacterial wall by the NP's adhesion, without apparently bacterial alteration by the high-dose of CuNPs exposition. The above corroborates that bacterial adaptation protects the bacterial structure, developing possible defense mechanisms, as observed by the pyocyanin production (Fig. 5).

Finally, we conclude that CuNPs demonstrate antibacterial behavior against *P. aeruginosa*, with a possible adaptation mechanism after the consecutive bacterial exposition, demonstrated by the combined overproduction of pyocyanin associated with oxidative stress and the genomic alterations in the DNA sequences of resistant bacteria. As a result, the proposed bacterial adaptation mechanism of extremophile *P. aeruginosa* NEJ08 induced by the interaction with CuNPs is presented in Fig. 8. The above opens the panorama to developing new strategies to design novel antimicrobials capable of avoiding the intrinsic bacterial resistance generated by the pathogen microorganisms.

ACKNOWLEDGEMENTS

This work was supported by CONACYT Mexico through the CB project A1-S-17842 *"Proyectos apoyados por el Fondo Sectorial de Investigación para la Educación."* K.G. Quintero-Garrido acknowledges CIDETEQ and CONACYT for the scholarship granted No. 31662. In addition, the support of CONACYT through grant 315178, *"Laboratorio Nacional en innovación y Desarrollo de Materiales Ligeros para la Industria Automotriz"* (LANI-AUTO), is greatly appreciated.

CONFLICT OF INTEREST

The authors have no conflict of interest to declare.

REFERENCES

Alonso, B., Fernández-Barat, L., Di Domenico, E.G., Marín, M., Cercenado, E., Merino, I., de Pablos, M., Muñoz, P., Guembe, M. 2020. Characterization of the virulence of *Pseudomonas aeruginosa* strains causing ventilator-associated pneumonia. BMC Infectious Diseases 20, 1–8. https://doi.org/10.1186/S12879-020-05534-1/FIGURES/2.

Amaro, F., Morón, Á., Díaz, S., Martín-González, A., Gutiérrez, J.C., 2021. Metallic Nanoparticles-Friends or Foes in the Battle against Antibiotic-Resistant Bacteria? Microorganisms, Vol. 9, Page 364 9, 364. https://doi.org/10.3390/MICROORGANISMS9020364.

Atalah, J., Espina, G., Blamey, L., Muñoz-Ibacache, S.A., Blamey, J.M., 2022. Advantages of Using Extremophilic Bacteria for the Biosynthesis of Metallic Nanoparticles and Its Potential for Rare Earth Element Recovery. Frontiers in Microbiology 13, 855077. https://doi.org/10.3389/FMICB.2022.855077.

Bacame-Valenzuela, F.J., Alberto Pérez-García, J., Castañeda-Zaldivar, F., Reyes-Vidal, Y., 2020. Pyocyanin biosynthesis by Pseudomonas aeruginosa using a biodiesel by product. Mexican Journal of Biotechnology, 1–16. https://doi.org/10.29267/mxjb.2020.5.3.1.

Benassai, E., Del Bubba, M., Ancillotti, C., Colzi, I., Gonnelli, C., Calisi, N., Salvatici, M.C., Casalone, E., Ristori, S., 2021. Green and cost-effective synthesis of copper nanoparticles by extracts of non-edible and waste plant materials from Vaccinium species: Characterization and antimicrobial activity. Materials Science and Engineering: C, 119, 111453. https://doi.org/10.1016/J.MSEC.2020.111453.

El-Fouly, M.Z., Sharaf, A.M., Shahin, A.A.M., El-Bialy, H.A., Omara, A.M.A., 2015. Biosynthesis of pyocyanin pigment by *Pseudomonas aeruginosa*. Journal of Radiation Research and Applied Sciences 8, 36–48. https://doi.org/10.1016/J.JRRAS.2014.10.007.

España-Sánchez, B. L., Ávila-Orta, C. A., Padilla-Vaca, F., Díaz Barriga-Castro, E., Soriano-Corral, F., González-Morones, P., Ramírez-Wong, D. G., Luna-Bárcenas, G., 2018. Early Stages of Antibacterial Damage of Metallic Nanoparticles by TEM and STEM-HAADF. Current Nanoscience 14 (1), 54-61. https://doi.org/10.2174/2468187307666170906150731.

Essar, D.W., Eberly, L., Hadero, A., Crawford, I.P., 1990. Identification and characterization of genes for a second anthranilate synthase in *Pseudomonas aeruginosa*: interchangeability of the two anthranilate synthases and evolutionary implications. Journal of Bacteriology 172, 884–900. https://doi.org/10.1128/JB.172.2.884-900.1990.

Evans, A. & Kavanagh, K.A., 2021. Evaluation of metal-based antimicrobial compounds for the treatment of bacterial pathogens. Journal of Medical Microbiology 70, 1363. https://doi.org/10.1099/JMM.0.001363.

Fariba, F., Bahram, G.E., Farrokh, K., Tabrizy, S., Pooneh, S. S., 2016. An Investigation of the Effect of Copper Oxide and Silver Nanoparticles on *E. Coli* Genome by Rapd Molecular Markers. Advances in Biotechnology & Microbiology. 1 (2). 10.19080/AIBM.2016.01.555559.

Fariña, N., 2016. Bacterial resistance. A global public health problem with difficult solution. Memorias del Instituto de Investigación en Ciencias de la Salud 14, 06–07. https://doi.org/10.18004/MEM.IICS/1812-9528/2016.014(01)06-007.

Ghasemian, E., Naghoni; Ali, Rahvar, H., Kialha, M., Tabaraie, B., Naghoni, A., 2015. Evaluating the Effect of Copper Nanoparticles in Inhibiting *Pseudomonas aeruginosa* and *Listeria monocytogenes* Biofilm Formation. Jundishapur Journal of Microbiology, 85, 8 (5), 17430. https://doi.org/10.5812/JJM.17430.

Govind, V., Bharadwaj, S., Sai Ganesh, M.R., Vishnu, J., Shankar, K. V., Shankar, B., Rajesh, R., 2021. Antiviral properties of copper and its alloys to inactivate covid-19 virus: a review. Biometals 34, 1217. https://doi.org/10.1007/S10534-021-00339-4.

Gu, H., Chen, X., Chen, F., Zhou, X., Parsaee, Z., 2018. Ultrasound-assisted biosynthesis of CuO-NPs using brown alga Cystoseira trinodis: Characterization, photocatalytic AOP,

DPPH scavenging and antibacterial investigations. Ultrasonics Sonochemistry 41, 109–119. https://doi.org/10.1016/J.ULTSONCH.2017.09.006.

Guzmán, K., Kumar, B., Vallejo, M.J., Grijalva, M., Debut, A., Cumbal, L., 2019. Ultrasound-assisted synthesis and antibacterial activity of gallic acid-chitosan modified silver nanoparticles. Progress in Organic Coatings 129, 229–235. https://doi.org/10.1016/J.PORGCOAT.2019.01.009.

Hall, S., McDermott, C., Anoopkumar-Dukie, S., McFarland, A.J., Forbes, A., Perkins, A. V., Davey, A.K., Chess-Williams, R., Kiefel, M.J., Arora, D., Grant, G.D., 2016. Cellular Effects of Pyocyanin, a Secreted Virulence Factor of *Pseudomonas aeruginosa*. Toxins 8 (8), 236. https://doi.org/10.3390/TOXINS8080236.

Humphreys-Salas, Z., Martínez-Ávila, A. F., Hernández-Orozco, M. A Elizalde-Peña, E.A., Palma-Tirado, L., Baldenegro-Pérez, L. A., Padilla-Vaca, F., Luna-Bárcenas, G., España-Sánchez, B. L. 2022. Green synthesis of copper nanoparticles and their formulation into face masks: An antibacterial study. Polymer Composites 43, 13. https://doi.org/10.1002/PC.27142.

Jabłońska, J., Dubrowska, K., Augustyniak, A., Wróbel, R.J., Piz, M., Cendrowski, K., Rakoczy, R., 2022. The influence of nanomaterials on pyocyanin production by *Pseudomonas aeruginosa*. Applied Nanoscience 12, 1929–1940. https://doi.org/10.1007/S13204-022-02461-2.

Jones, R.N., Pfaller, M.A., 1998. Bacterial Resistance: A Worldwide Problem. Diagnostic Microbiology and Infectious Disease 31 (2), 379–388. https://doi.org/10.1016/S0732-8893(98)00037-6.

Kaur, P., Thakur, R., Chaudhury, A., 2016. Biogenesis of copper nanoparticles using peel extract of *Punica granatum* and their antimicrobial activity against opportunistic pathogens 9 (1), 33–38. https://doi.org/10.1080/17518253.2016.1141238.

Keihan, A.H., Veisi, H., Veasi, H., 2017. Green synthesis and characterization of spherical copper nanoparticles as organometallic antibacterial agent. Applied Organometallic Chemistry 31 (7), e3642. https://doi.org/10.1002/AOC.3642.

Laehnemann, D., Peña-Miller, R., Rosenstiel, P., Beardmore, R., Jansen, G., Schulenburg, H., 2014. Genomics of Rapid Adaptation to Antibiotics: Convergent Evolution and Scalable Sequence Amplification. Genome Biology and Evolution 6 (6), 1287–1301. https://doi.org/10.1093/GBE/EVU106.

LewisOscar, F., MubarakAli, D., Nithya, C., Priyanka, R., Gopinath, V., Alharbi, N.S., Thajuddin, N., 2015. One pot synthesis and anti-biofilm potential of copper nanoparticles (CuNPs) against clinical strains of *Pseudomonas aeruginosa*. Biofuling 31 (4), 379–391. https://doi.org/10.1080/08927014.2015.1048686.

Marques, C. R., 2018. Extremophilic Microfactories: Application in Metal and Radionuclide Bioremediation. Frontiers in Microbiology 9, 1191. https://doi.org/10.3389/fmicb.2018.01191.

McNeilly, O., Mann, R., Hamidian, M., Gunawan, C., 2021. Emerging Concern for Silver Nanoparticle Resistance in *Acinetobacter baumannii* and Other Bacteria. Frontiers in Microbiology 12, 894. https://doi.org/10.3389/FMICB.2021.652863/BIBTEX.

Mubeen, B., Ansar, A.N., Rasool, R., Ullah, I., Imam, S.S., Alshehri, S., Ghoneim, M.M., Alzarea, S.I., Nadeem, M.S., Kazmi, I., 2021. Nanotechnology as a Novel Approach in Combating Microbes Providing an Alternative to Antibiotics. Antibiotics 10 (12), 1473. https://doi.org/10.3390/ANTIBIOTICS10121473.

Muller, M., Merrett, N.D., 2014. Pyocyanin Production by *Pseudomonas aeruginosa* Confers Resistance to Ionic Silver. Antimicrobial Agents and Chemotherapy 58 (9), 5492-5499. https://doi.org/10.1128/AAC.03069-14.

Muñoz-Escobar, A., Reyes-López, S.Y., 2020. Antifungal susceptibility of *Candida* species to copper oxide nanoparticles on polycaprolactone fibers (PCL-CuONPs). PLoS One 15, e0228864. https://doi.org/10.1371/JOURNAL.PONE.0228864.

Niño-Martínez, N., Salas Orozco, M.F., Martínez-Castañón, G.A., Méndez, F.T., Ruiz, F., 2019. Molecular Mechanisms of Bacterial Resistance to Metal and Metal Oxide Nanoparticles. International Journal of Molecular Sciences 20 (11), 2808. https://doi.org/10.3390/IJMS20112808.

Panáček, A., Kvítek, L., Smékalová, M., Večeřová, R., Kolář, M., Röderová, M., Dyčka, F., Šebela, M., Prucek, R., Tomanec, O., Zbořil, R., 2018. Bacterial resistance to silver nanoparticles and how to overcome it. Nature Nanotechnology 13, 65–71. https://doi.org/10.1038/s41565-017-0013-y.

Romano, I., Vitiello, G., Gallucci, N., Girolamo, R. D., Cattaneo, A., Poli, A., Donato, P. D. 2022. Extremophilic Microorganisms for the Green Synthesis of Antibacterial Nanoparticles. Microorganisms 10 (10), 1885. https://doi.org/10.3390/MICROORGANISMS10101885.

Salah, I., Parkin, I.P., Allan, E., 2021. Copper as an antimicrobial agent: recent advances. RSC Advances 11, 18179–18186. https://doi.org/10.1039/D1RA02149D.

Sánchez-López, E., Gomes, D., Esteruelas, G., Bonilla, L., Lopez-Machado, A.L., Galindo, R., Cano, A., Espina, M., Ettcheto, M., Camins, A., Silva, A.M., Durazzo, A., Santini, A., Garcia, M.L., Souto, E.B., 2020. Metal-Based Nanoparticles as Antimicrobial Agents: An Overview. Nanomaterials 10 (2), 292. https://doi.org/10.3390/NANO10020292.

Tkachenko, A.G., 2018. Stress Responses of Bacterial Cells as Mechanism of Development of Antibiotic Tolerance (Review). Applied Biochemistry and Microbiology 54, 108–127. https://doi.org/10.1134/S0003683818020114.

Whooley, M.A. & McLoughlin, A.J., 1982. The regulation of pyocyanin production in *Pseudomonas aeruginosa*. European Journal of Applied Microbiology and Biotechnology 15, 161–166. https://doi.org/10.1007/BF00511241.

Zangeneh, M.M., Ghaneialvar, H., Akbaribazm, M., Ghanimatdan, M., Abbasi, N., Goorani, S., Pirabbasi, E., Zangeneh, A., 2019. Novel synthesis of *Falcaria vulgaris* leaf

extract conjugated copper nanoparticles with potent cytotoxicity, antioxidant, antifungal, antibacterial, and cutaneous wound healing activities under *in vitro* and *in vivo* condition. Journal of Photochemistry and Photobiology B: Biology 197, 111556. https://doi.org/10.1016/J.JPHOTOBIOL.2019.111556.

Zhang, S., Wang, Y., Song, H., Lu, J., Yuan, Z., Guo, J., 2019. Copper nanoparticles and copper ions promote horizontal transfer of plasmid-mediated multi-antibiotic resistance genes across bacterial genera. Environment International 129, 478–487. https://doi.org/10.1016/J.ENVINT.2019.05.054.